Available online at www.sciencedirect.com
ScienceDirect
Catalysis Today 121 (2007) 246–254
CATALYSIS TODAY
www.elsevier.com/locate/cattod

The measurement of gas diffusivity in porous materials by temporal analysis of products (TAP)

Wenjun Li [a], Lanying Xie [b], Lei Gao [a], Xueliang Zhao [a], Rongrong Hu [a], Yi Cheng [a], Dezheng Wang [a,*]

[a] Department of Chemical Engineering, Tsinghua University, Beijing 100084, China
[b] Research Center, Changde Cigarette Manufacture Company, Tongyan Road West, Changde, Hunan 415000, China

Available online 6 September 2006

Abstract

The pulsing of argon in a temporal analysis of products (TAP) reactor and reactor modeling of the response curves were used to measure the effective intraparticle diffusivities in porous materials. The diffusivity that can be measured is limited: (1) at the low end by intraparticle diffusion being too slow such that just a small fraction of the pulse gets into the pores to give an indistinguishable tail, which only measures that the diffusivity is smaller than an upper limit and (2) at the high end by intraparticle diffusion being too fast such that it gives a constant concentration in the pores, which only measures that the diffusivity is larger than a lower limit. The limits and range are slightly different for different particle and bed dimensions. A 9 mm long packed bed has a sensitive range of about 300-fold where there are discernible changes in the normalized pulse shape due to diffusivity changes. If small particles of about 50 μm are used, the range is from 1×10^{-10} to 3×10^{-8} m^2/s, and if large particles of about 500 μm are used, the range is from 2×10^{-9} to 5×10^{-7} m^2/s.

Keywords: Intraparticle diffusivity; Porous powder; TAP reactor; Diffusivity measurement; Diffusion

1. Introduction

The dependence of the intraparticle diffusivity on the molecular species is useful for separation and catalyst selectivity control using porous materials. The measurement of the intraparticle diffusivity is important in these uses. Readily available techniques for measuring gas diffusivity in porous materials include permeability, Wilke–Kallenbach, time lag, sorption rate measurement, efficiency factor, frequency response and chromatographic methods [1–4]. These are macroscopic techniques in contrast to the microscopic techniques of pulsed-field gradient (PFG) NMR and quasielastic neutron scattering that directly detect diffusing molecules and use the Einstein random-walk model.

Many researchers [1,2,5] have lamented the large differences in the measured diffusivities reported in the literature, especially in the measurements by the macroscopic and microscopic methods. Nijhuis et al. [6] pointed out that microscopic techniques generally give faster diffusivities and lower activation energies while macroscopic techniques generally give higher activation energies and slower diffusivities. They suggested that external heat and mass transport may influence the measurement in the macroscopic methods and may not have been correctly accounted for. The microscopic methods directly measure the movement of diffusing molecules inside the pores and therefore are not coupled to transport processes outside the pores. Another suggested cause of the discrepancy is the different timescales of the macroscopic and microscopic methods: PFG-NMR measurements take a few milliseconds while most macroscopic techniques take many minutes and can give different diffusivities if only a fraction of sorbed molecules is mobile [2]. The differences may also be real and the techniques differ in a fundamental way that is as yet unknown [1,2].

A new method to measure diffusivity in porous materials is to use the temporal analysis of products (TAP) reactor. This was pioneered by Nijhuis et al. [6] and Keipert and Baerns [7]. Nijhuis et al. [6] presented results that agree with those from PFG-NMR, and concluded that although this is a macroscopic technique (the measured quantities are the concentrations

* Corresponding author. Tel.: +86 10 62794468; fax: +86 10 6277 2051.
E-mail address: wangdz@flotu.org (D. Wang).

0920-5861/$ – see front matter © 2006 Elsevier B.V. All rights reserved.
doi:10.1016/j.cattod.2006.07.020

Nomenclature

$A(x)$	cross-sectional area of reactor at axial position x (m^2)
C_i	gas phase concentration of species i (mol/m^3)
$D_{bed,i}(x)$	effective diffusivity of species i in a packed bed at axial position x (m^2/s)
$D_{par}(r)$	effective diffusivity of species i in a porous spherical particle (m^2/s)
D_{MS}	effective diffusivity of species i in the quadrupole mass filters (m^2/s)
$D_{void,i}(x)$	effective diffusivity of species i in void space at axial position x (m^2/s)
L_x	TAP apparatus diffusion length (m)
$N_{p,i}$	species i input pulse (mol/s)
q_i	gas phase concentration of species i in the porous particles (mol/m^3)
$\bar{q}_i$	average gas phase concentration of species i in porous particles (mol/m^3)
l	length variable in the quadrupole mass filters (m)
r	radial variable of the porous particle (m)
r_{par}	radius of the particles (m)
s_i	gas phase concentration of species i in quadrupole mass filters (mol/m^3)
$\bar{s}_i$	average gas concentration of species i in quadrupole mass filters (mol/m^3)
t	time from the gas injection (s)
x	space variable in the reactor (one-dimensional model) (m)
$\delta(t-\tau)$	Dirac function (at time τ), dimensionless
ε_b	catalyst bed void fraction, dimensionless
ε_s	fraction of gas species that did not diffuse into the quadrupole mass filters

outside the pores and the processes during the measurements include the transport of molecules in the packed bed prior to transport into the particles), the TAP technique apparently is more like a microscopic technique. They explained this as due to the TAP reactor's operation under vacuum where the transport of molecules through the bed is by Knudsen diffusion, which avoids external transport effects.

However, the diffusivity of comparable systems measured by a TAP reactor reported by different groups [6–11] can differ by more than 10-fold. Also, Brandani and Ruthven [8] have raised some questions on the TAP technique, which were addressed by Nijhuis et al. within the framework of their methodology. Although the TAP reactor is potentially a fast and easy way to measure diffusivity uncomplicated by interparticle mass and heat transport, there are significant differences in the models used in different research groups [6–12] showing that its methodology has not yet been fully agreed upon. In this work, the reactor modeling, precision and sensitivity of the measurements, and some experimental precautions that should be taken are further discussed. Most works have considered sorption in zeolites, which includes adsorption, desorption, and probably configurational diffusion, in addition to Knudsen diffusion, while this work considers just the Knudsen diffusion of an inert gas, which is a simpler system more suitable for discussing the methodology. The experiments are performed in the diffusion regime where only the Knudsen mechanism is important, and the analysis does not need to consider mixed mechanisms.

The TAP reactor is very convenient because it works well with ordinary powder samples, which obviates the need for large crystalline samples. It can be viewed as a variant of the transient Wilke–Kallenbach method in which a packed bed is the pellet in the diffusion cell or a variant of the chromatographic technique. It can be expected to be more useful because its experiments are easy and its operation is as convenient as in the chromatographic technique. More important is that its transient response curves are independent of the flow and highly reproducible. The timescale of the experiments is 100 ms–5 s and it may form a basis to resolve the differences between the microscopic and macroscopic techniques.

2. Experimental

The apparatus is basically a packed bed into which a pulse of inert argon is introduced. The transient response that elutes from the packed bed (TAP curve) is measured. Reactor simulation and non-linear regression are used to extract the diffusivity parameters using as data the spread of the pulse due to diffusion in the bed and intraparticle diffusion in the catalyst pellets. The apparatus differs from and has advantages over those in the transient Wilke–Kallenbach and chromatographic techniques in that it is operated in the Knudsen flow regime, which is achieved by using very small gas pulses injected into an evacuated reactor. This is advantageous because the mathematical modeling is much simpler and exact since Knudsen flow and its diffusion coefficient (Knudsen diffusivity) are physically well defined.

The experiments were carried out in a reactor based on the TAP reactor described by Gleaves et al. [13]. The reactor uses solenoid valves for gas input. The sample was placed in a 4 mm i.d., 110 mm long stainless steel, cylindrical tube as a packed bed held in place by wire screens. The detector is RGA 200 quadrupole mass spectrometers factory-modified to use external fast response current amplifiers (SRS, USA). There are two mass spectrometers placed in a cylindrical vacuum chamber of 30 cm diameter and 57 cm long. One end of the chamber is sealed except for a small hole to receive gases from the reactor outlet. The ionizers of the mass spectrometers and the small hole are aligned along the axis of the chamber. The other end of the chamber is open and flanged to the entrance of a $1500\ l\ s^{-1}$ turbomolecular pump. Collected data were usually signal averaged over five pulses.

The powders used were γAl_2O_3, active carbon, glass beads and SiC. The particle sizes of the samples were determined using a Master Sizer Micro-Plus 50 particle size apparatus from Malvern (England). BET areas and pore size distributions (PSD) were measured using adsorption manometry. The γAl_2O_3 is type 13-2525 from Strem Chemicals (USA). It has 185 m^2/g BET area and was sieved to give particle sizes

with a roughly Gaussian distribution with a full width at half maximum (FWHM) of 40 μm centered at 85 μm. Its pores have a roughly Gaussian PSD with a FWHM of 3.0 nm centered at 5.5 nm. The active carbon is from Shanxi Taiyuan Active Carbon Factory. It has 748 m^2/g BET area and was sieved to particle sizes with a roughly Gaussian distribution with a FWHM of 200 μm centered at 370 μm. Its pores have a PSD with a FWHM of 0.60 nm centered at 1.3 nm. The glass beads are from Beijing Guanghua Thermal Materials Factory produced by a vapor spray process that gives narrow size distributions for various size fractions. These are non-porous. They were used in various sieved fractions in the range of 7–250 μm diameter. The SiC particles were from Jiangsu Nantongyuda Silicon Carbide Company and were used after grinding and sieving. The gas used was commercial purified argon.

In the reactor simulation and parameter estimation, the numerical integration of the partial differential equations used the Crank–Nicholson scheme. Parameter fitting was sometimes performed with the Nelder–Mead or simulated annealing algorithms, but more usually was performed manually using visual inspection of the curves to optimize the parameters. The accuracy of the numerical computation was verified by halving time and space steps until the results agree on visual inspection. Generally, a space step of 0.1 mm and a time step of 0.01 ms were used.

3. Mathematical model

TAP reactor modeling has already been well discussed. Here, a brief description is given of where the model here is different and to discuss points relevant to the modeling of intraparticle diffusion in porous particles. The model is a packed bed of porous particles in a cylindrical tube. The reactor continuity equation for gas species is the diffusion equation with source/sink terms [6–13]. For diffusion into and out from the particles, the source/sink is due to the accumulation or depletion of the gas species in the particles. The pore structure of the particles is not modeled explicitly, that is, a pseudo-homogeneous porous particle model is used. Using the L_x defined in Fig. 1, the continuity equation for a gas species is written as:

$$\frac{\partial C_i}{\partial t} = \frac{1}{A(x)}\frac{\partial}{\partial x}A(x)D_{\text{void},i}(x)\frac{\partial C_i}{\partial x} \quad \text{for } 0 \le x < L_1,$$
$$L_2 \le x < L_3,\ L_3 \le x < L_4,\ L_5 \le x \le L_6 \tag{1a}$$

$$\varepsilon_b \frac{\partial C_i}{\partial t} = \frac{1}{A(x)}\frac{\partial}{\partial x}A(x)D_{\text{bed},i}(x)\frac{\partial C_i}{\partial x} - (1-\varepsilon_b)\frac{\partial \bar{q}_i}{\partial t} \tag{1b}$$
$$\text{for } L_1 \le x < L_2$$

$$\varepsilon_s \frac{\partial C_i}{\partial t} = \frac{1}{A(x)}\frac{\partial}{\partial x}A(x)D_{\text{void},i}(x)\frac{\partial C_i}{\partial x} - (1-\varepsilon_s)\frac{\partial \bar{s}_i}{\partial t} \tag{1c}$$
$$\text{for } L_4 \le x < L_5$$

The presence of zones where the diffusivity and/or diameter are different is accounted for by the use of $A(x)$ and $D_{\text{bed},i}(x)$ as functions of position. It has been verified [14] that this form of the continuity equation gives TAP curves similar to those from the more conventional TAP form that uses the boundary conditions of the conservation of flux and concentration at the zone boundaries. The last term on the right hand side of Eq. (1b) is the diffusion of the gas species into/out of the porous particles in the packed bed, and of (1c) is the diffusion of the gas species into/out of the quadrupole mass filters that are modeled as dead end diffusion tubes, respectively. The initial condition and boundary conditions for Eqs. (1a)–(1c) are:

$$0 \le x \le L = \text{vacuum pump entrance},$$
$$t = 0, \quad C_i = 0; \quad \forall i \tag{2}$$

$$x = 0, \quad t \ge 0,$$
$$-D_{void,i}(0)A(0)\left.\frac{\partial C_i}{\partial x}\right|_0 = \delta(t-\tau)N_{\text{p,i}}(\delta\text{-function pulse}) \tag{3}$$

$$x = L = \text{vacuum pump entrance}, \quad t \ge 0,$$
$$-D_{void,i}(L)A(L)\left.\frac{\partial C_i}{\partial x}\right|_L = S_p C_i|_L \tag{4}$$

The method used in the modeling is to develop the reactor model and fit its parameters using the TAP curves for Knudsen flow in empty tubes of various lengths [15] where the physical theory is well defined. These parameters are then held fixed for all subsequent simulations, e.g., the estimation of the effective intraparticle diffusivity parameter. The model here is different in the use of boundary condition (4) and the modeling of a mass spectrometer as a diffusion tube. These were introduced to resolve the observation that the experimental TAP curves of empty tubes were broader than the simulated TAP curves when the reactor model was that used in the older works [6–13], which was used with the value for the Knudsen diffusivity of the tubes calculated from the kinetic theory of gases.

Boundary condition (4) differs from that used in other works [6–13] that specify that the gas concentration at the reactor exit is zero. Boundary condition (4) accounts for the situation that the vacuum pump has a finite pumping speed. With this boundary condition, Eqs. (1a)–(1c) includes the vacuum

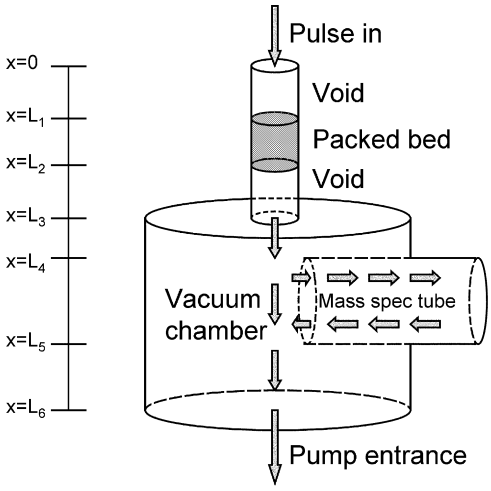

Fig. 1. Schematic diagram of the flow path.

chamber, as shown in Fig. 1, because the concentration there is non-zero, that is, it describes a diffusion path that is from the point of pulse injection through the reactor tube and vacuum chamber to the inlet of the vacuum pump. In Eq. (4), S_p is the pumping speed and is a parameter fitted using the TAP curves of empty tubes of various lengths [15] that is then held constant for all other simulations. The use of boundary condition (4) also indicates that the TAP curve is the concentration-time curve at the position of the mass spectrometer, and this also differs from other works [6–13] where the TAP curve is the flux from the reactor exit. Both these differences, that the gas pulse stays for a finite time in the vacuum chamber and the mass spectrometer measures the concentration and not the flux, cause changes in the shape of the simulated TAP response curve.

The method is similar to that used by Delgrado et al. [16] who have also reported similar observations with empty tubes, namely, that the experimental TAP curve is broader than the simulated TAP curve when the reactor model is roughly similar to that used in the older works [6–13]. They modified the conventional model with the use of surface roughness (which was a fitted parameter to give a reduction in the Knudsen diffusivity) and a finite pumping speed (and the vacuum chamber modeled as a CSTR) to account for the broadened TAP curve. The modification here of the conventional model differs from Delgrado et al. in four aspects: (1) surface roughness is not invoked, which is due to the experimental result that the TAP curves were not much different with a new good quality stainless steel (ss) tube, a used ss tube that looks ''rough'', and a quartz tube, (2) the vacuum chamber is treated as a diffusion tube instead of a CSTR, (3) the pumping speed is a fitted parameter, which is slightly less than the manufacturer's rated pumping speed, and (4) the mass spectrometer is treated as a diffusion tube where the diffusivity is a fitted parameter. The reactor model used here gave good fits for Knudsen flow in empty tubes of various lengths [15] and measured a Knudsen diffusivity that is in good agreement with that calculated by the kinetic theory of gases. With the old boundary condition that aft of the reactor exit, the concentration is zero, the modeling of empty tubes of various lengths gave Knudsen diffusivities that varied with the lengths and were 40–60% of the Knudsen formula, and for tubes less than 70 mm, even the shapes of the response curves could not be fitted.

The continuity equation inside the pseudo-homogeneous porous particles is:

$$\frac{\partial q_i}{\partial t} = \frac{1}{r^2}\frac{\partial}{\partial r} r^2 D_{\text{par}} \frac{\partial q_i}{\partial r} + \text{adsorption/desorption terms} \tag{5}$$

Eq. (5) is coupled to Eqs. (1a)–(1c) through the last term on the right hand side of Eq. (1b). The initial condition for Eq. (5) is:

$$0 < r \le r_{\text{par}}, \quad t = 0, \quad q_i = 0 \tag{6}$$

The boundary conditions for Eq. (5) are:

$$r = 0, \quad t \ge 0, \quad -\frac{\partial q_i}{\partial r} = 0 \tag{7}$$

$$r = r_{\text{par}}, \quad t > 0, \quad q_i = C_i \tag{8}$$

Boundary condition (8) uses the existence of Knudsen flow where there is no external resistance around the particle. This differs from works that use Henry's law: $q_i = K_H C_i$, that model diffusion in zeolite crystals [5–9] where the sorption situation in the particle was described as a one-phase system, or where adsorption was assumed fast, and D_{par} in Eq. (5) is to be interpreted as an apparent diffusivity [3].

The average concentration in the particles, used to compute the source/sink term in Eqs. (1a)–(1c), is:

$$\bar{q}_i(x,t) = \frac{1}{\frac{4}{3}\pi r^3} 4\pi \int_0^{r_{\text{par}}} q_i r^2 \mathrm{d}r \tag{9}$$

This work uses a different form for the sink/source term due to diffusion into and out of the particles. Most workers use the flux through the outer surface of the particles: $(1-\varepsilon_b)\frac{3}{r_p} D_{\text{pore}} \frac{\partial q_i}{\partial r}\big|_{r_p}$. This work uses the form in Kärger and Ruthven [1]: $(1-\varepsilon_b)\frac{\partial \bar{q}_i}{\partial t}$, which is the time rate of change of the average concentration in the porous particle (cf. Eqs. (1b) and (9)). The two forms should be equal, and are equal in the experiments simulated here. But for fast transients, their computational accuracy can be different, and numerical experiments indicate that it is computationally more demanding to compute the flux at the outer surface. This may be because it is calculated as a differential whereas the change in the average concentration is calculated by integration.

The continuity equation inside the mass spectrometer quadrupole mass filter is:

$$\frac{\partial s_i}{\partial t} = D_{\text{MS}} \frac{\partial^2 s_i}{\partial l^2} \tag{10}$$

Eq. (10) is coupled to Eqs. (1a)–(1c) through the last term on the right hand side of Eq. (1c). Eq. (10) is supplemented by equations similar to Eqs. (6)–(9), with obvious changes in notation and geometry.

4. Results and discussion

The operation of the reactor under Knudsen flow is the physical basis of the model and for the advantage that the technique is not subject to external transport limitations (there is no boundary layer film around the particle in Knudsen flow). The experimental condition that ensures Knudsen flow is that the pressure in the reactor is low enough. This was satisfied with the use of very small pulses. The pulses used were generally less than 2×10^{15} molecules per pulse, and when necessary were varied in the range 3×10^{13} to 2×10^{15} molecules per pulse.

The most convenient experimental method to verify Knudsen flow is to show that the normalized TAP curves are independent of the pulse size [13]. This is the case with all the results reported here for pulse sizes that were varied over 60-fold from 3×10^{13} to 2×10^{15} molecules. This shows that the diffusivity is independent of pressure, and since Knudsen flow is the only flow regime where the diffusivity is independent of pressure, it proves the existence of Knudsen flow. Other characteristics of Knudsen flow are: the normalized response

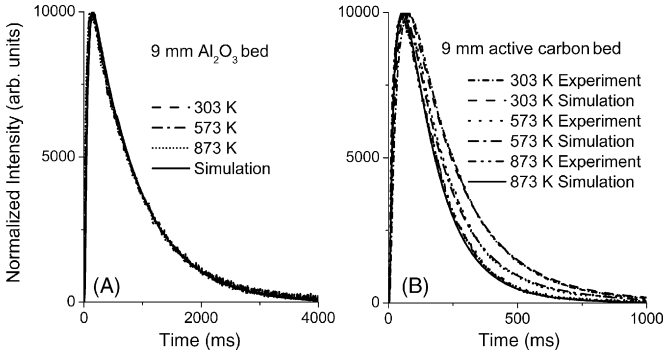

Fig. 2. TAP curves from 9 mm beds of porous γAl_2O_3 and active carbon powder at different temperatures.

curves are independent of the gas compositions, Knudsen number > 1, and the measured diffusivity (measured in the experiments with the empty tubes) agrees with that calculated from kinetic theory (and it scales with the diameter, and varies as the square root of temperature and inverse molecular mass).

The system used satisfied all these characteristics except that the bed diffusivity of the powder samples often did not vary as the square root of the temperature. Fig. 2 shows the TAP curves for 9 mm long, 4 mm diameter packed beds of γAl_2O_3 and active carbon as a function of temperature. The diffusivity of the γAl_2O_3 bed is virtually unchanged with temperature. The fitted diffusivities of the 9 mm active carbon bed are 0.00288, 0.00332, 0.00368, 0.00404, and 0.00444 m^2/s at 30, 150, 300, 450, and 600 °C, respectively. Using the diffusivity at 30 °C as the base, the Knudsen temperature dependence should give the diffusivity as 0.00340, 0.00396, 0.00444, and 0.00489 m^2/s at 150, 300, 450, and 600 °C, respectively. In this case, the measured Knudsen diffusivities are about 10% smaller than the temperature extrapolated values. However, the difference can vary with many factors, with an apparent trend as follow: (1) in a stainless steel tube, the diffusivity of γAl_2O_3 powders hardly varied with temperature, while short beds of active carbon and SiC showed some weak dependence on temperature and long beds of these powders can get close to obeying the Knudsen dependence on temperature, and (2) in a quartz tube, the diffusivities of γAl_2O_3 powders show some dependence on temperature that is weaker than square root, while short beds of active carbon powders get close to obeying the square root Knudsen dependence on temperature and long beds of this powder can show a stronger than a square root dependence on temperature.

At the moment, this is presented as an experimental observation with the cause not understood. An unfortunate implication is that the temperature of the bed may be not well defined. Due to this, the results reported here are for experiments at room temperature. For the γAl_2O_3 packed bed, it was verified that there was an increase in bed temperature by placing materials that undergo an irreversible color change on reaching a certain temperature in the bed and confirming that these materials were changed. Also, reactions that should occur at certain temperatures of the γAl_2O_3 bed, e.g., dehydration, do occur.

In these experiments, the γAl_2O_3 packed bed, where most of the pulse broadening occurred, was positioned in the constant temperature zone of the heater. Outside of the constant temperature zone, there were zones with temperature gradients where the temperature decreased to the cooling water temperature at the vacuum seals. The presence of zones with a temperature gradient would affect a TAP curve through the temperature dependence of the Knudsen diffusivity and thermal transpiration. These effects are expected to be small here because the diffusivity in these zones (void space) is much larger than in the γAl_2O_3 packed bed and the results of Delgrado et al. [16] indicate that the effect of thermal transpiration will be small here. Thus, although the presence of temperature gradients can change the TAP curve shape, this effect is not enough to explain the above results.

A characteristic of Knudsen flow is that the diffusivity scales with a characteristic length. For a packed bed, the particle diameter is the characteristic length. Fig. 3 shows the bed diffusivity for packed beds of glass bead of different sizes in a 4 mm i.d. tube. The correlation of the bed diffusivity with the particle size is linear, in agreement with the kinetic theory of Knudsen flow. The correlation in Fig. 3 does not pass through the origin. This is probably due to entrance effects since the length/diameter ratios of the packed beds are not large. Fig. 3 was used to get the bed diffusivity to reduce the number of fitted parameters in the simulations.

In this work, the fitted parameters were effectively reduced to just the parameter of interest, namely, the effective intraparticle diffusivity in the porous sample by the use of a three-part parameter fitting process. The first part used four TAP curves from four empty tubes that were 40, 70, 100, and 140 mm long, respectively, to establish the parameters of the vacuum chamber. Four parameters were fitted, which are: diffusivity of void space, pumping speed at the vacuum pump entrance, and the fraction of gas that diffuses into and the diffusivity inside the quadruple mass filters. A diffusivity of void space proportional to the diameter, in accordance with the Knudsen formula, was used so that one parameter that use the relevant diameters sufficed for the empty tube and the vacuum chamber diffusivities. The flow path dimensions inside the

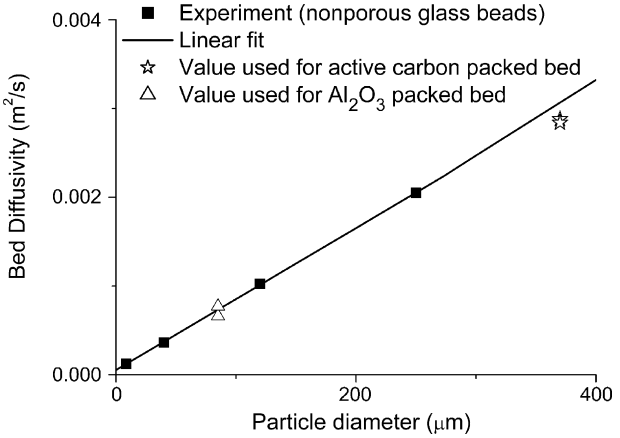

Fig. 3. Effective diffusivities of packed beds of different sized non-porous glass beads.

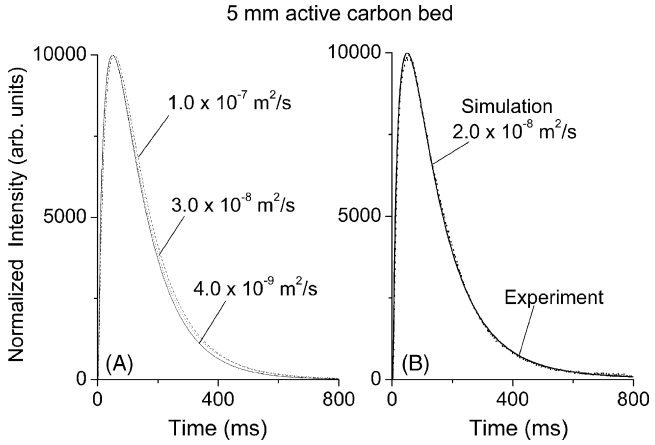

Fig. 4. TAP curves of a 5 mm bed of 370 μm porous active carbon powder. (A) Simulated curves to show the range of D_{par} where the normalized curves have different shapes. (B) Experimental (dotted) TAP curve and the best fit (solid) curve with D_{par} as the adjustable parameter.

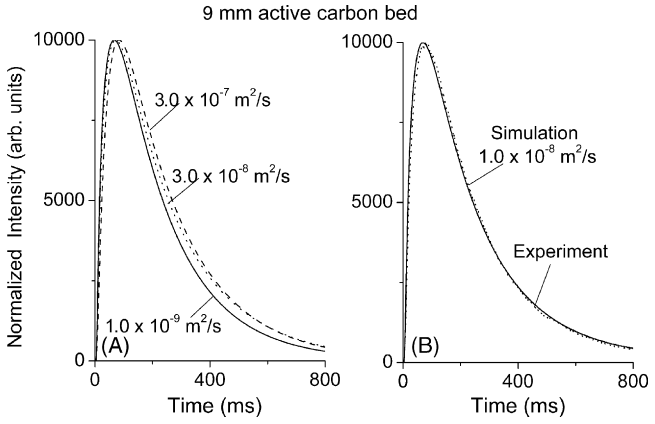

Fig. 5. TAP curves of a 9 mm bed of 370 μm porous active carbon powder. (A) Simulated curves to show the range of D_{par} where the normalized curves have different shapes. (B) Experimental (dotted) TAP curve and the best fit (solid) curve with D_{par} as the adjustable parameter.

quadruple mass filters are not known and the diffusivity there was a fitted parameter. These parameters were subsequently fixed. The dimensions of the reactor and vacuum chamber were measured quantities. The fits were good and the fitted void diffusivity was within 5% of the Knudsen formula [15]. The diffusivity of void space used was $130d_r$ m^2/s where d_r (in m) is the diameter at position x.

The second part of the parameter fitting established Fig. 3, which is a correlation between the bed effective diffusivity and particle size of the packed bed. This used a number of packed beds comprising different sized fractions of non-porous glass beads. For each packed bed comprising glass beads of a fixed size fraction, one parameter (bed effective diffusivity) was fitted. This correlation was used to give the third part of the parameter fitting below a bed diffusivity that was subsequently ''quasi-fixed'' in the sense that it was allowed to change in a narrow range of ±10% of the correlation to reflect that a packed bed cannot be exactly reproduced with respect to the packing (void fraction). Usually, the final value used was close to the value derived from Fig. 3 if the shape of the porous particle is close to that of the glass bead used to acquire Fig. 3. In Fig. 3, the values actually used in the third part are also shown.

The third part of the parameter fitting used the data from a packed bed of the porous powder whose intraparticle diffusivity was being measured. For each specific powder sample, one parameter (powder effective internal diffusivity) was fitted, with a second quasi-fixed parameter (bed effective diffusivity) being allowed to change in a range of ±10%. The methodology is similar to that of Delgrado et al. [9] who fitted and fixed the parameters of the vacuum system and reactor using an empty tube.

Figs. 4–7 show how simulated TAP curves change as a function of the effective intraparticle diffusivity (D_{par}), and some data and examples of the quality of the parameter-optimized fit of D_{par}. Fig. 4 shows the curves for a 5 mm packed bed of 370 μm active carbon powder. Fig. 4A shows simulated TAP curves for D_{par} from 4.0×10^{-9} to 1.0×10^{-7} m^2/s. For $D_{par} \geq 1.0 \times 10^{-7}$ m^2/s and $D_{par} \leq 4.0 \times 10^{-9}$ m^2/s, the TAP curves do not differ. Numerical simulations show that at the high end, intraparticle diffusion is fast and there is negligible intraparticle concentration gradient, while at the low end, intraparticle diffusion is too slow and there is negligible concentration inside the particle. At the low end, the situation here is different from that of sorption in a zeolite crystal because there is no adsorption, and the range of D_{par} where the TAP curves are discernibly different is much smaller (about 25-fold in Fig. 4A). Also, within this range, the TAP curves, although different, do not show large changes in normalized shapes. The fitted and experimental curves in Fig. 4B and a comparison with Fig. 4A show that the changes are sufficient to allow the fitting of D_{par}, but the precision is not high. The fitted D_{par} is estimated as in the range 1–4 $\times 10^{-8}$ m^2/s. This range is based on the visual inspection of how much D_{par} can change before it is clearly seen that the simulated curve differs from the experimental curve. It should be noted that the fitting is possible only because the TAP experimental curve is highly

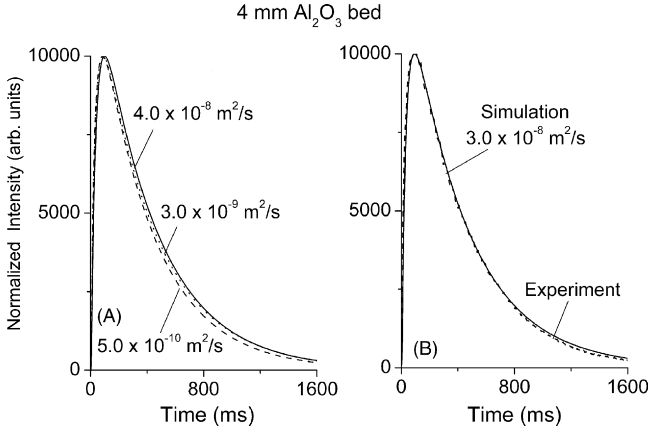

Fig. 6. TAP curves of a 4 mm bed of 85 μm porous γAl_2O_3 powder. (A) Simulated curves to show the range of D_{par} where the normalized curves have different shapes. (B) Experimental (dotted) TAP curve and the best fit (solid) curve with D_{par} as the adjustable parameter.

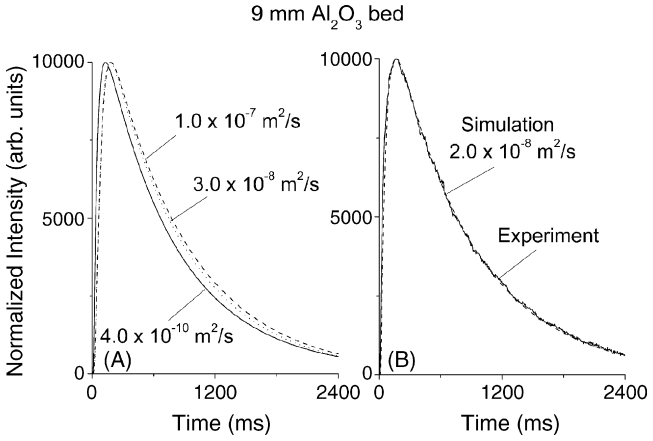

Fig. 7. TAP curves of a 9 mm bed of 85 μm porous γAl_2O_3 powder. (A) Simulated curves to show the range of D_{par} where the normalized curves have different shapes. (B) Experimental (dotted) TAP curve and the best fit (solid) curve with D_{par} as the adjustable parameter.

reproducible. It will be discussed below that errors in the experiment procedure can lead to quite different values of D_{par}.

The low precision in Fig. 4 is due to the use of a short packed bed. Fig. 5 shows the curves for a longer 9 mm packed bed. There is improved resolution, that is, the TAP curves show larger changes as D_{par} changes, in particular, the peak of the curve shows a more distinct shift to later time as a faster intraparticle diffusion results in more gas getting into the particle. Marin and co-workers [17] have shown that in a single zone model, when intraparticle diffusion is fast such that there is negligible intraparticle concentration gradient, the TAP curve of a porous powder bed is the same as that of a non-porous powder bed with a smaller bed diffusivity. This is not true in a multi-zone TAP reactor, that is, the TAP curve of a porous powder bed is different in normalized shape from that of a non-porous powder bed, but the trend is the same, that is, there is a shift of the curve peak to later time and a worker who is not aware that this is a porous powder bed may try to fit the curve with a smaller bed diffusivity. In Fig. 5A, the bed diffusivity is constant and the intraparticle diffusivity is varied. It can also be seen that the range of D_{par} where the TAP curves are discernible has increased to about 300-fold. The fitted D_{par} is estimated to be in the range 1–2×10^{-8} m^2/s.

Figs. 6 and 7 show the curves for 4 and 9 mm packed beds of 85 μm γAl_2O_3 powder to show the situation with a smaller powder. Figs. 6A and 7A again show that the range of D_{par} where the TAP curves differ is larger and the differences in the curves are larger with the longer bed. Figs. 6B and 7B show the experimental and fitted curves to show that the fits are acceptable. From Fig. 7B, the fitted D_{par} is estimated to be in the range 2.5–3.5×10^{-8} m^2/s.

Many workers have commented that the diffusion time, L^2/D, is a characteristic of a diffusion system that can be used as a guide for choosing the system dimensions for measuring the diffusivity. For the 370 μm active carbon powder, the diffusion times were 0.029, 0.094, and 3.4 s for the 5 mm bed, 9 mm bed, and intraparticle diffusion, respectively. For the 85 μm γAl_2O_3 powder, the diffusion times were 0.081, 0.35, and 0.090 s for the 4 mm bed, 9 mm bed, and intraparticle diffusion, respectively. Based on these numbers, however, it should be argued that the diffusion times give only a very rough guide. If one uses the diffusion times as a guide, one would consider grinding the active carbon to a smaller size to get more compatible diffusion times, but simulations show this does not give better precision and there can be a serious problem grinding can cause that is discussed below. Although the diffusion times for the active carbon powder do not seem quite compatible, the fitted D_{par} is roughly in the middle of the sensitive range, where the precision is higher. On the other hand, the diffusion times for the γAl_2O_3 powder, esp. with the 4 mm bed, seem compatible, but the fitted D_{par} is near to the (lower) limit of the sensitive range where the TAP curves show less change with varying D_{par}. It appears that the use of simulations is more useful as a guide for choosing the dimensions of the packed bed.

With a large particle (such as the active carbon powder), the bed diffusivity is large and it might seem that longer beds will give better precision in fitting D_{par}, but in our system, 10 mm is about the maximum length that should be used. When the packed bed is longer, the TAP curves can sometimes become not reproducible over a long time period in the sense that although TAP curves measured a few days apart are reproducible, those measured a long time apart may be slightly different. The reason for this is not yet understood.

Conversely, for a small powder (such as the γAl_2O_3 powder), the problem is that the intraparticle diffusion time is very short, but the bed diffusivity is small, which causes the pulse to stay in the bed longer. It might seem that a shorter bed [9] will be better for fitting D_{par}, but a shorter bed will have a larger error in the measurement. The use of structured powders [9] may be useful. Alternatively, it may seem that grinding and compacting the powder to a larger size will allow the use of a longer bed, but there can be a serious problem grinding can cause that is discussed below.

The fitted D_{par} for the active carbon powder is 1–2×10^{-8} m^2/s. The estimated effective intraparticle diffusivity is 1.7×10^{-8} m^2/s, when estimated using the pore size of 1.3 nm and calculating with the Knudsen formula and the textbook guideline that the ε/τ factor is 0.1 [18]. The fitted D_{par} for the γAl_2O_3 powder is 2.5–3.5×10^{-8} m^2/s. The estimated effective intraparticle diffusivity by the textbook guideline is 7.3×10^{-8} m^2/s. This indicates that it is preferable to experimentally measure the effective intraparticle diffusivity, if possible. From Figs. 4–7 and the discussion above, it is estimated that the TAP technique can measure diffusivity in the range 1×10^{-10} to 5×10^{-7} m^2/s, if it is possible to use a 9 mm bed of very small particles of 50 μm to measure the diffusivity in the range from 1×10^{-10} to 3×10^{-8} m^2/s, and to use a 9 mm bed of large particles of about 500 μm to measure the diffusivity in the range from 2×10^{-9} to 5×10^{-7} m^2/s. If it is just possible to use particles of only one size, the use of a 9 mm packed bed will give a measurable range of about 300-fold where the location of the range depends on the particle size.

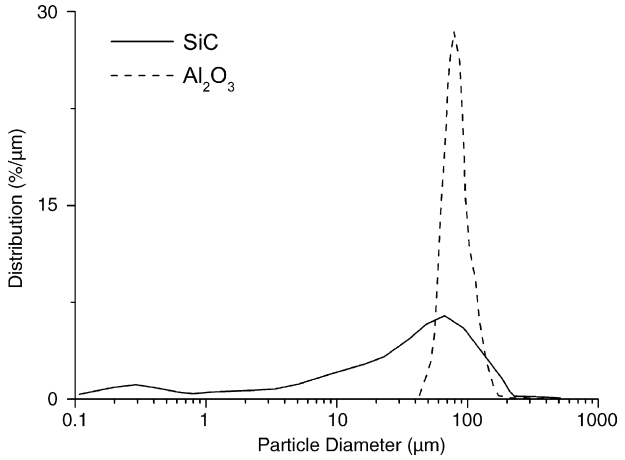

Fig. 8. Particle size distributions of sieved porous γAl_2O_3 powder and ground and sieved SiC powder measured by a Master Sizer Micro-Plus 50 (Malvern, England).

In many TAP experiments that use a small powder, a packed bed made of the original powder will have a small bed diffusivity and give very broad TAP curves, e.g., Fig. 7. It is common practice to grind and compact the small powder to a larger size to give good looking TAP curves. This procedure can cause wrong estimates of D_{par}. Fig. 8 shows the measured particle distribution of our SiC powder to show the source of the problem. The SiC powder was used after grinding and sieving to a narrow mesh range. The sieving should select out a fraction with a narrow size range, but Fig. 8 shows that the sieved powder has a wide size distribution with a fair proportion of very small particles. A detailed analysis indicated that the problem was that the grinding resulted in some very small particles. Such small particles have a tendency to agglomerate because of their high surface energy, and they form agglomerates of a large size that behave as large particles in the sieve. However, the diffusion behavior of these agglomerates is that of their constituent very small particles. Fig. 9 compares the TAP curves of packed beds of the SiC and γAl_2O_3 powder that have the size distributions shown in Fig. 8. The two powders were sieved to the same mesh fraction and should have the same size, but it can be seen that the SiC beds have broader TAP curves than the γAl_2O_3 powder beds despite the fact that the SiC is non-porous and the γAl_2O_3 is porous. The size distribution data in Fig. 8 suggest that the explanation is that the presence of very small SiC powders have broadened the TAP curve and caused tailing.

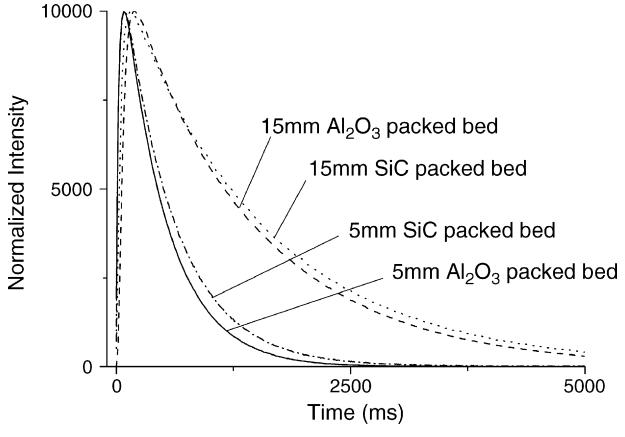

Fig. 9. TAP curves of packed beds of sieved porous γAl_2O_3 powder and ground and sieved SiC powder with the size distributions in Fig. 8.

In a previous work where the γAl_2O_3 powder was first ground and compacted, the resulting TAP curves also showed a similar broadening and tailing, but which was not accounted for, and that gave an intraparticle diffusivity that was 10 times smaller than the ones reported here. Thus, care must be taken to ensure that the particles comprising the packed bed do not have a wide particle size distribution, but this does not imply the need for a particle size distribution so narrow that it is difficult to get. Sieving can give a particle size distribution that is narrow enough to be satisfactory provided the particles were not severely ground beforehand and do not contain fines that are liable to form agglomerates. If there is any doubt about whether a wide particle size distribution may be present, sieving should not be relied upon to guarantee this, but observations should be made with a particle size apparatus.

5. Conclusion

Pulse experiments in a TAP reactor can be used to measure the effective intraparticle diffusivity in porous materials to give more realistic values compared to the estimates made using the rules of thumb from the literature. A 9 mm long packed bed has a sensitive range of about 300-fold change in the diffusivity where there are discernible changes in the TAP curve shape. With small particles of about 50 μm, the range is from 1×10^{-10} to 3×10^{-8} m^2/s, and with large particles of about 500 μm, the range is from 2×10^{-9} to 5×10^{-7} m^2/s. Simulations can be used to choose suitable dimensions. The temperature dependence of the Knudsen diffusivity of a TAP reactor packed bed can differ from that of the Knudsen formula. The reason is not yet known. The use of ground material may lead to mistaken results due to the presence of small particles that agglomerate to form large agglomerates that appear to a sieve as large particles.

Acknowledgements

This work is supported by the Ministry of Science and Technology, China (No. 2005CB221405) and the National Natural Science Foundation (China) (grant 20273036).

References

[1] J. Kärger, D.M. Ruthven, Diffusion in Zeolites and Other Microporous Solids, Wiley/Interscience, New York, 1992.
[2] N.Y. Chen, T.F. Degnan Jr., C.M. Smith, Molecular Transport and Reaction in Zeolites, VCH, New York, 1994.
[3] H.W. Haynes Jr., Catal. Rev. Sci. Eng. 30 (1988) 563.
[4] S.T. Kolaczkowski, Catal. Today 83 (2003) 85.
[5] F. Kapteijn, W.J.W. Bakker, G. Zheng, J.A. Moulijn, Microporous Mater. 3 (1994) 227.

[6] T.A. Nijhuis, L.J.P. van den Broeke, J.M. van de Graaf, F. Kaptiijn, M. Makkee, J.A. Moulijn, Chem. Eng. Sci. 52 (1997) 3401.
[7] O.P. Keipert, M. Baerns, Chem. Eng. Sci. 53 (1998) 3623.
[8] S. Brandani, D. Ruthven, Chem. Eng. Sci. 55 (2000) 1935.
[9] J.A. Delgado, T.A. Nijhuis, F. Kapteijn, J.A. Moulijn, Chem. Eng. Sci. 59 (2004) 2477.
[10] A.H.J. Colaris, J.H.B.J. Hoebink, M.H.J.M. de Croon, J.C. Schouten, Am. Inst. Chem. Eng. J. 48 (2002) 2587.
[11] A.C. van Veen, D. Farrusseng, M. Rebeilleau, T. Decamp, A. Holzwarth, Y. Schuurman, C. Mirodatos, J. Catal. 216 (2003) 135.
[12] D.Z. Wang, F.X. Li, X.L. Zhao, Chem. Eng. Sci. 59 (2004) 5615.
[13] J.T. Gleaves, J.R. Ebner, T.C. Kuechler, Catal. Rev. Sci. Eng. 30 (1988) 49.
[14] D.Z. Wang, J. Chin. Chem. Soc. 50 (2003) 551.
[15] L. Gao, X.L. Zhao, D.Z. Wang, Stud. Surf. Catal. 159 (2006) 677.
[16] J.A. Delgado, T.A. Nijhuis, F. Kapteijn, J.A. Moulijn, Chem. Eng. Sci. 57 (2002) 1835.
[17] J.P. Huinink, J.H.B.J. Hoebink, G.B. Marin, Can. J. Chem. Eng. 74 (1996) 580.
[18] J.B. Butt, Reaction Kinetics and Reactor Design, second ed., Marcel Dekker, New York, 2000.